Electronic Supplementary Material (ESI) for Physical Chemistry Chemical Physics.

$CuZrO_3$: If it exists it should be a sandwich

James Dean, Yahui Yang, Götz Veser, Giannis Mpourmpakis*

Department of Chemical Engineering, University of Pittsburgh, Pittsburgh PA 15213, USA

*Corresponding Author Email: gmpourmp@pitt.edu

Structural Tolerance Factors

In this work, we use the set of ionic radii published by Shannon[1]. We assign a charge of +4 to Zr and -2 to O, on the basis that this is their typical oxidation state. Cu is then required to be in its common +2 state to achieve a per-formula-unit neutral charge. We take the ionic radius of O^{2-} in the coordination number (CN) 8 tips of the octahedra to be 1.42 Å.

In the case where Zr^{4+} is in the CN12 A-site and Cu^{2+} is in the CN6 B-site, we encounter a challenge: the A site should have 12-fold coordination with neighboring oxygen atoms, yet the Shannon data for Zr^{4+} is only available for CN 4 – 9. For this, we estimate the ionic radius of this species by doing a first order linear regression on CN versus ionic radius, yielding $r_{Zr} \approx 0.06CN + 0.3567$ (R^2 = 0.998). We then extrapolate to CN12 and use the value 1.0767 Å for the ionic radius of Zr^{4+}. CN6 Cu^{2+}, on the other hand, has a tabulated value: 0.73 Å.

In the case where Cu^{2+} is in the CN12 A-site and Zr^{4+} is in the CN6 B-site, we run into a similar challenge, where the Shannon data is only available for CN 4, 5, and 6. This yields $r_{Cu} \approx 0.08CN + 0.25$ $(R^2 = 1.000)$, which results in an ionic radius of 1.21 Å for CN12 Cu^{2+}. CN6 Zr^{4+}, however, has a tabulated value of 0.72 Å.

Goldschmidt

The Goldschmidt tolerance factor (Equation 1) is a well-known relation used to determine whether a compound with the ABX_3 formula will form a perovskite. A and B are the two cations, typically metals, and X is the anion, usually either a chalcogenide or halide.

$$t = \frac{r_A + r_X}{\sqrt{2}(r_B + r_X)} \quad (1)$$

In equation 1, r_N represents the ionic radius of the species in the CN12 A-site, the CN6 B-site, or the CN8 chalcogen/halogen atom.

With Zr^{4+} in the A-site, this results in t = 0.82.

With Cu^{2+} in the A-site, this results in t = 0.87.

Bartel

The tolerance factor of Bartel et al[2] takes the form found in Equation 2. The variables used are the same as Goldschmidt's equation, with t being replaced by tau, and the addition of a n_N term representing the oxidation state of species n. In this equation, "X" refers to an oxidizing species typically from the nitrogen, chalcogen, or halogen group (in our case, O).

$$\tau = \frac{r_X}{r_B} - n_A\left(n_A - \frac{\frac{r_A}{r_B}}{\ln\left(\frac{r_A}{r_B}\right)}\right) \quad (2)$$

With Zr^{4+} in the A-site ($n_A = 4$), this results in τ = 1.13.

With Cu^{2+} in the A-site ($n_A = 2$), this results in τ = 4.45.

DFT Optimization of Experimental CuO and ZrO_2

For the purposes of calculating the decomposition energy of the reaction $CuZrO_3 \rightarrow CuO + ZrO_2$, the unit cells of CuO and ZrO_2 were investigated using Density Functional Theory (DFT). We utilize the Vienna Ab-initio Simulation Package (VASP)[3] in conjunction with the PBE functional[4] and PAW potentials[5]. A gamma-centered mesh of 5x5x5 k-points is used. A planewave cutoff of 500 eV is used, with an SCF convergence criterion of 10^{-5} eV. Geometry optimizations proceeded with a convergence criterion of 10^{-4} eV/ Å, allowing the atomic coordinates and cell dimensions to optimize simultaneously.

CuO

The experimental structure of CuO[6] (Tenorite) was obtained from the Open Quantum Materials Database (OQMD)[7, 8] (entry 671141), which itself was obtained from the literature[6]. This was then optimized. A comparison of the unit cell parameters of the optimized cell (Figure S1) and experiment can be found in Table S1.

Table S1. Unit cell parameters for DFT-optimized and experimental CuO. Note that in both cases, the reduced (i.e. primitive) unit cell determined by VESTA[9] is reported.

PARAMETER	DFT OPTIMIZED	EXPERIMENT
A	2.942 Å	2.884 Å
B	2.942 Å	2.884 Å
C	5.166 Å	5.108 Å
α	87.555°	82.366°
β	87.555°	82.366°
γ	80.786°	72.472°

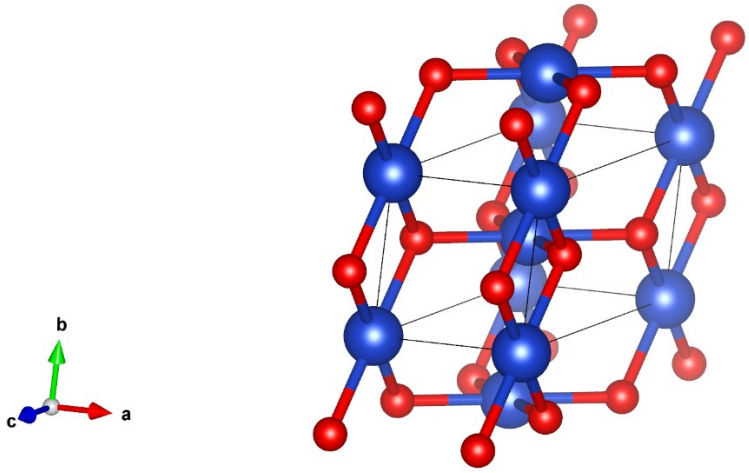

Figure S1. Optimized structure of CuO. Key: Blue=Cu, red=O.

ZrO_2

The experimental structure of monoclinic ZrO_2[10] (Baddeleyite) was obtained from the OQMD (entry 3278), which itself had been obtained from the literature[10]. A comparison of the unit cell parameters and the optimized cell (Figure S2) can be found in Table S2. The electronic energy of the converged unit cell is calculated to be -114.285 eV. With 4 formula units in the unit cell, this results to -28.571 eV / formula unit.

Table S2. Unit cell parameters of the DFT-optimized and experimental ZrO_2. Note that in both cases, the reduced (i.e. primitive) unit cell determined by VESTA[9] is reported.

PARAMETER	DFT OPTIMIZED	EXPERIMENT
A	5.115 Å	5.210 Å
B	5.118 Å	5.260 Å
C	5.116 Å	5.370 Å
α	90.000°	90.000°
β	90.171°	99.470°
γ	90.000°	90.000°

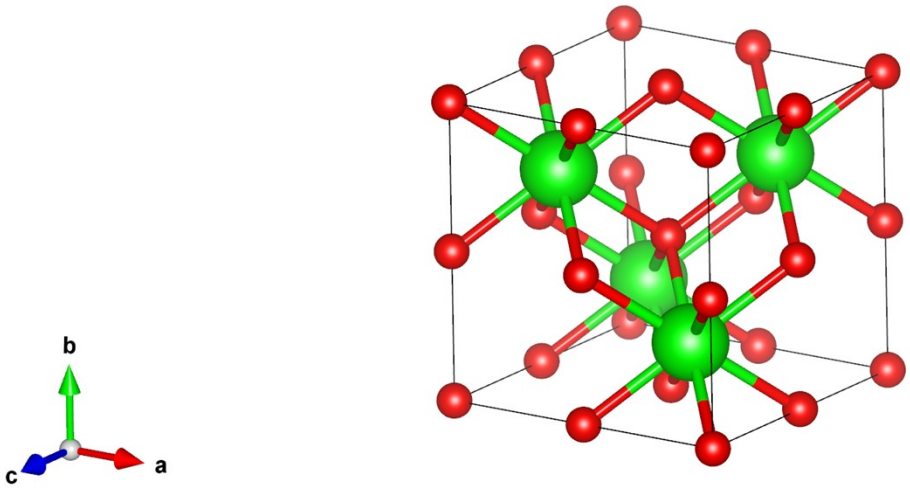

Figure S2. Optimized structure of monoclinic ZrO_2. Key: Green=Zr, red=O.

Unit Cell Predictions

A variety of unit cells were considered in our investigation of the structure of $CuZrO_3$. The structure name convention and energetic data can be found in Table S3.

Table S3. Unit cell electronic energy and decomposition energy in eV per formula unit. The table is sorted by decomposition energy. The naming convention used throughout the manuscript follows "Source – ID." For example, structure ea430 from USPEX would be reported as USPEX-ea430.

Source	ID	Formula	Number of Formula Units	Energy (eV/unit)	Decomposition (eV/Unit)
USPEX	ea430	$Cu_2O_6Zr_2$	2	-38.19	-0.42
USPEX	ea480	$Cu_4O_{12}Zr_4$	4	-37.94	-0.68
Perovskite Protype (Zr-Oct)	D	$Cu_4O_{12}Zr_4$	4	-37.91	-0.70
Materials Project	1140859	$Cu_4O_{12}Zr_4$	4	-37.83	-0.79
Perovskite Protype (Cu-Oct)	B	$Cu_4O_{12}Zr_4$	4	-37.77	-0.84
Perovskite Protype (Cu-Oct)	E	$Cu_4O_{12}Zr_4$	4	-37.75	-0.86
Materials Project	1140852	$Cu_8O_{24}Zr_8$	8	-37.74	-0.88
Perovskite Protype (Cu-Oct)	C	$Cu_4O_{12}Zr_4$	4	-37.72	-0.90
Materials Project	1140850	$Cu_6O_{18}Zr_6$	6	-37.71	-0.90
Perovskite Protype (Cu-Oct)	A	$Cu_4O_{12}Zr_4$	4	-37.71	-0.90
Perovskite Protype (Cu-Oct)	F	$Cu_4O_{12}Zr_4$	4	-37.70	-0.92

USPEX	ea247	$Cu_7O_{21}Zr_7$	7	-37.70	-0.92
Perovskite Protype (Cu-Oct)	D	$Cu_4O_{12}Zr_4$	4	-37.68	-0.94
Perovskite Protype (Zr-Oct)	F	$Cu_4O_{12}Zr_4$	4	-37.63	-0.98
Perovskite Protype (Zr-Oct)	C	$Cu_4O_{12}Zr_4$	4	-37.59	-1.02
Perovskite Protype (Zr-Oct)	E	$Cu_4O_{12}Zr_4$	4	-37.59	-1.02
Perovskite Protype (Zr-Oct)	A	$Cu_4O_{12}Zr_4$	4	-37.59	-1.02
Materials Project	1140851	$Cu_2O_6Zr_2$	2	-37.26	-1.36
Perovskite Protype (Zr-Oct)	B	$Cu_4O_{12}Zr_4$	4	-37.23	-1.39
Materials Project	1140866	$Cu_2O_6Zr_2$	2	-37.05	-1.56
OQMD	354456	CuO_3Zr	1	-35.06	-3.56
OQMD	352285	CuO_3Zr	1	-33.33	-5.28

Deviation from the Perovskite System

While investigating the “Perovskite Prototype (Zr-Oct) D” system presented in Table S3, we observe a large deviation from the initial perovskite structure. As this was the third-most-favorable system, and the first in which a perovskite was used as an initial structural guess, we investigate it in greater detail. Over the course of the geometry optimization, the Cu cations have migrated to form square planes connecting the edges of the Zr octahedra (depicted in Figure S3). In the fully-optimized system (Figure S3 D) we find the arrangement of octahedra joined at the vertices typically seen in perovskites, although the A-site cations (Cu) have moved into a 4-fold planar coordination with neighboring O atoms.

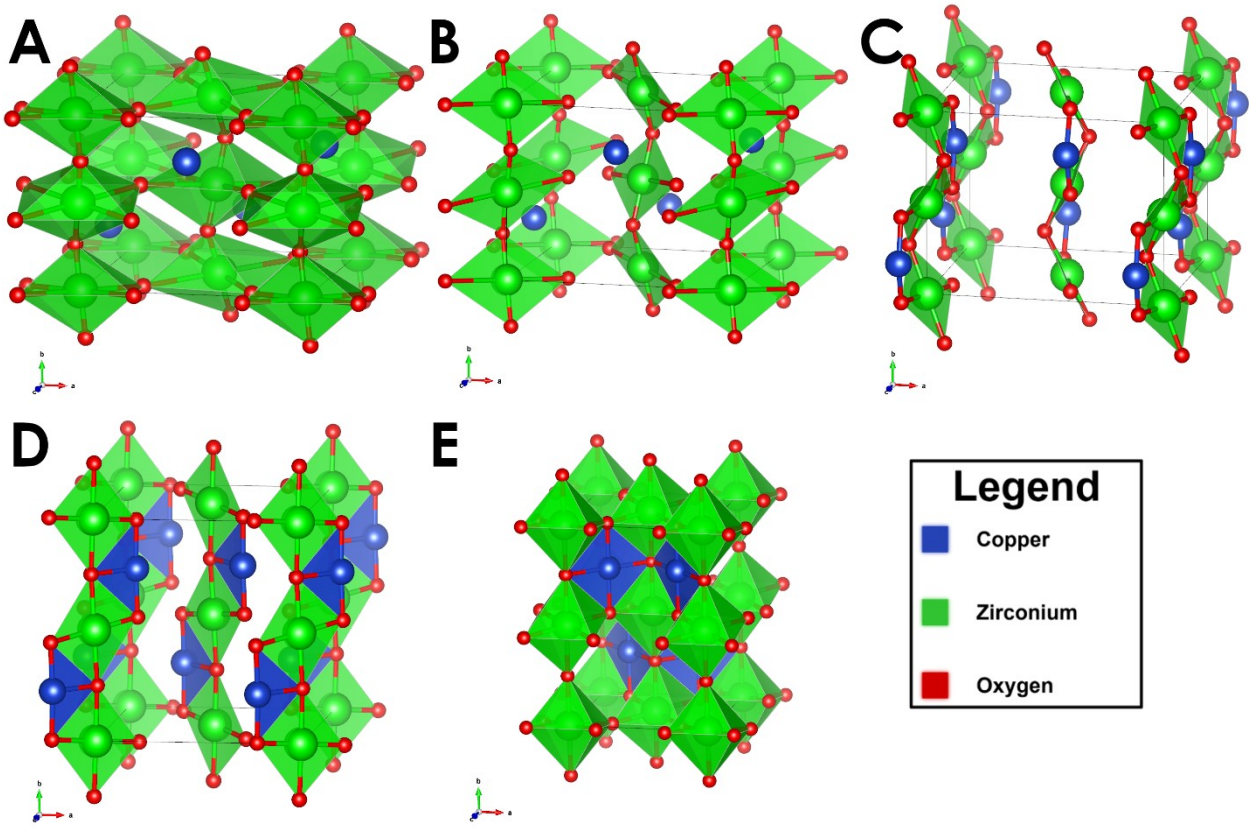

Figure S3. Evolution of the "Perovskite Prototype (Zr-Oct)-D" structural prototype during optimization. Structures are presented chronologically with respect to the optimization process. (A) The initial structural guess. (B) Input to an atomic coordinates optimization following a coarse-grained volume relaxation. (C) Optimization result of atomic coordinates relaxation with cell-vectors frozen. (D) Optimization result of the constant-volume relaxation of cell-vectors and atomic coordinates. (E) Optimization result where cell vectors and atomic coordinates are allowed to relax without restriction. The unit cell in all cases is drawn with black lines. Key: Blue=Cu, Green=Zr, Red=O.

In contrast, and of interest, is that the OQMD perovskites (which remained perovskites throughout the optimization) were by far the least stable systems (see Table S3), with decomposition energies of -5.28 eV/formula unit when Cu is the B-size cation, and -3.56 when Zr is the B-site cation (see Figure S4). Thus, out of all the systems we have investigated so far, a perovskite structure is the least favorable – and the “Perovskite Prototype” system, which began as a perovskite, deviated from the perovskite structure when the geometry was optimized.

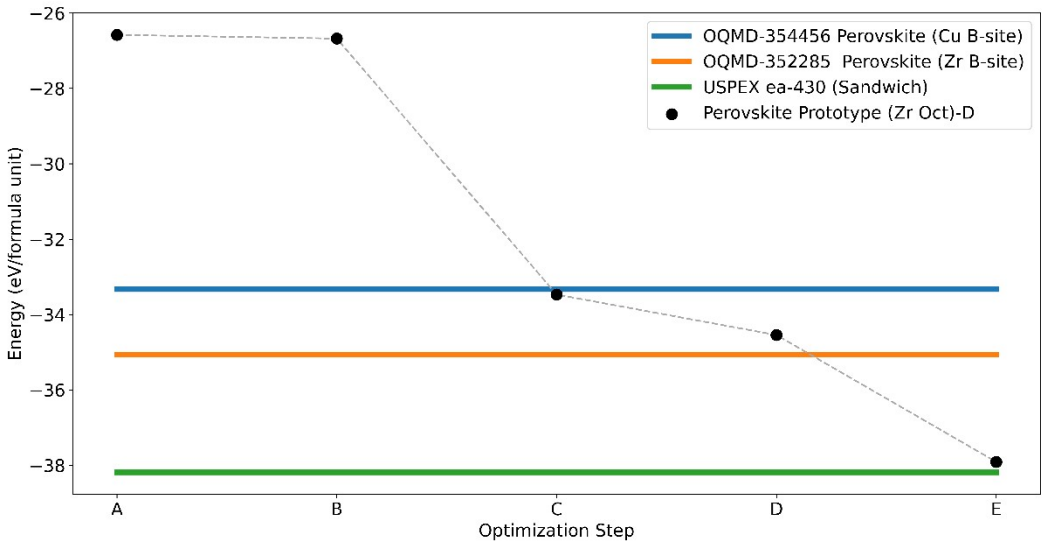

Figure S4. Optimization trajectory of the perovskite prototype (Zr-Oct)-D. Ticks on the X-axis correspond with the labels of Figure S3 (e.g. the "C" structure is drawn Figure S3 C). As a reference, we have included the OQMD perovskites (blue and orange horizontal lines) and the Sandwich morphology (green horizontal line).

It is interesting to see this deviation from the perovskite cell occur inconstantly between systems. The likely reason for this is because unlike the OQMD systems, this prototype began life as essentially a 2x2x2 supercell of a perovskite unit cell, and thus had the freedom to deviate from the perovskite. In the case of the OQMD systems, they are essentially a 1x1x1 supercell of a perovskite unit cell (an ideal perovskite unit cell is presented in Figure 1).

PBE0 Comparison

We have also performed a limited set of PBE0[11] single point energy calculations, by first recalculating the electronic density via a single-point PBE calculation and then using this electron density as the initial guess for the single-point PBE0 calculation. The results of our single-point PBE0 calculations can be found in Table S4. Overall, we find that in the case of a single-point PBE0 calculation, the trend in decomposition energy preference reverses – the perovskite-prototype system (which we note had deviated from a perovskite structure during the course of PBE optimization; see Supporting Information section "Deviation from the Perovskite System" for more details) becomes more stable than the sandwich morphology, although it is still unstable (i.e. it has a negative decomposition energy).

Table S4. The results of PBE0 energy calculations for CuO, the Perovskite prototype, the Sandwich morphology (USPEX ea430), and ZrO_2. In this case, we report PBE-optimized systems for all systems, with single-point calculations performed at the PBE0 level.

Material	Number of Formula Units	PBE0 Energy (eV)	PBE0 Energy (eV/formula unit)	PBE0 Decomposition Energy to CuO+ZrO_2 (eV/formula unit)
CuO (PBE-optimized)	2	-24.40	-12.20	NA
Perovskite-prototype (PBE-optimized)	4	-196.00	-49.00	-0.06
Sandwich (PBE-optimized)	2	-97.27	-48.63	-0.43
ZrO_2 (PBE-optimized)	4	-147.45	-36.86	NA

We note, however, that this comparison was performed as a single-point PBE0 calculation on the PBE-optimized structure. As this flip in trend may be an artifact of the single point PBE0 calculation on the PBE-optimized geometry, we additionally attempted some geometry relaxations with the PBE0 functional. As this makes the SCF much more computationally-intensive to calculate, we only did this for the perovskite-prototype and sandwich morphologies. We find that the structure itself does not change much, although the energetic trends do change (Table S5).

Table S5. The results of PBE0 calculations for CuO, the Perovskite prototype, the Sandwich morphology (USPEX ea430), and ZrO_2. In this case, we report PBE0 optimized systems for the structural prototypes. The CuO and ZrO_2 were optimized with PBE and single-point calculations performed at the PBE0 level.

Material	Number of Formula Units	PBE0 Energy (eV)	PBE0 Energy (eV/formula unit)	PBE0 Decomposition Energy to CuO+ZrO_2 (eV/formula unit)
CuO (PBE-optimized)	2	-24.40	-12.20	N/A
Perovskite-prototype (PBE0-optimized)	4	-196.13	-49.03	-0.03
Sandwich (PBE0-optimized)	2	-98.57	-49.28	+0.22
ZrO_2 (PBE-optimized)	4	-147.45	-36.86	N/A

In the case of the perovskite prototype structure, we find the decomposition energy becomes -0.03 eV/formula unit, and in the case of the sandwich, we find it is +0.22 eV/formula unit (which would indicate that decomposition is disfavorable). We note here that due to the enhanced computational challenged posed by PBE0, we were only able to converge the perovskite-prototype to within a change in force of -0.03 eV/Å between steps 25 and 26 (within a period of 12 days using 224 cores).

References

1. R. Shannon, *Acta Crystallographica Section A*, 1976, **32**, 751-767.
2. C. J. Bartel, C. Sutton, B. R. Goldsmith, R. Ouyang, C. B. Musgrave, L. M. Ghiringhelli and M. Scheffler, *Sci Adv*, 2019, **5**, eaav0693.
3. G. Kresse and J. Furthmüller, *Physical Review B*, 1996, **54**, 11169-11186.
4. J. P. Perdew, K. Burke and M. Ernzerhof, *Physical Review Letters*, 1996, **77**, 3865-3868.
5. G. Kresse and D. Joubert, *Physical Review B*, 1999, **59**, 1758-1775.
6. G. Tunell, P. E and C. J. Ksanda, *Zeitschrift für Kristallographie - Crystalline Materials*, 1935, **90**, 120-142.
7. J. E. Saal, S. Kirklin, M. Aykol, B. Meredig and C. Wolverton, *JOM*, 2013, **65**, 1501-1509.
8. S. Kirklin, J. E. Saal, B. Meredig, A. Thompson, J. W. Doak, M. Aykol, S. Rühl and C. Wolverton, *Npj Computational Materials*, 2015, **1**, 15010.
9. K. Momma and F. Izumi, *Journal of Applied Crystallography*, 2011, **44**, 1272-1276.
10. N.-S. St. v, *Zeitschrift für Kristallographie - Crystalline Materials*, 1936, **94**, 414-416.
11. J. P. Perdew, M. Ernzerhof and K. Burke, *The Journal of Chemical Physics*, 1996, **105**, 9982-9985.